RSC Advances

ROYAL SOCIETY OF CHEMISTRY

PAPER

View Article Online
View Journal | View Issue

Cite this: *RSC Adv.*, 2023, **13**, 1203

Synthesis, characterization, and *in vitro* anti-cholinesterase screening of novel indole amines†

Humaira Yasmeen Gondal,[a] Sobia Tariq,[a] Shahzaib Akhter,[a] Abdul Rauf Raza,*[a] Muhammad Fayyaz ur Rehman*[a] and Syeda Laila Rubab[b]

Received 15th August 2022
Accepted 8th December 2022

DOI: 10.1039/d2ra05105b

rsc.li/rsc-advances

The present study involved the targeted synthesis and characterization of novel indole amines with anti-acetylcholinesterase profiling. A series of proposed indole amines was virtually screened against human acetylcholinesterase. A few indole amines (**23**, **24**, and **25**) showing strong enzyme binding in the *in silico* studies were synthesized in the laboratory and characterized using spectroscopic (IR, UV, NMR, single crystal XRD) and spectrometric (EIMS, HR-EIMS) methods. The indole amine **23** was crystallized from EtOH and analyzed with single crystal XRD. These ligands interacted with the PAS site in the enzyme, and their binding may disrupt the activity. The *in vitro* acetylcholinesterase inhibition studies revealed that the IC_{50} values for indole amines **25** and **24** (4.28 and 4.66 μM, respectively) were comparable to that of galantamine (4.15 μM) and may be studied further as cost-effective acetylcholinesterase inhibitors.

1. Introduction

The indole [2,3-benzo-(1*H*)-azole or 2,3-benzo-(1*H*)-pyrrole] is a remarkable class of heteroaromatic compounds that has been found in many natural products and has been a focus of numerous synthetic studies. The indole moiety found in natural products and synthetic compounds has gained popularity due to its various pharmacological activities, such as anti-cancer,[1] anti-tumor,[2] anti-proliferative,[3] anti-HIV,[4] anti-ulcer,[5] anti-parkinsonian,[6] anti-malarial,[7] anti-oxidant,[8] anti-inflammatory,[9] anti-viral,[10] anti-bacterial,[11] anti-fungal,[12] anti-MRSA,[13] anti-emetic,[14] anti-asthmatic, opioid agonist, sexual dysfunction,[15] anti-convulsant,[16] anti-migraine,[17] anti-depressant,[18] anti-obesity,[19] anti-hypertensive,[20] acetylcholinesterase inhibitory,[21] butyryl-cholinesterase inhibitory,[22] α-glucosidase inhibitory,[23] β-glucuronidase inhibitory,[24] α-amylase inhibitory,[25] and urease inhibitory.[26] It has recently been discovered that the indole acts as a signaling molecule in various roles, including plasmid stability, drug resistance, extracellular signaling, biofilm formation, and virulence control.[27]

Alzheimer's Disease (AD) is the condition of progressive dementia diagnosed by the loss of cognitive function and memory. It has been found that there is an accumulation of plaque within the brain of AD patients due to the accumulated beta-amyloids and neurofibrillary tangles (NFTs).[28] Some enzymes, such as acetylcholinesterase (AChE), glycogen synthase kinase 3 (GSK3), cyclin-dependent kinase 5 (CDK5), and secretase, as well as the *N*-methyl-D-aspartate (NMDA) receptor, play a role in the progression of this disease.[29] AD symptoms are alleviated if the levels of the neurotransmitter acetylcholine (ACh) are increased by inhibiting AChE. Higher AChE activity promotes the aggregation of Aβ plaques and neurofibrillary tangles within the brain.[30] FDA-approved drugs such as memantine (*N*-methyl-D-aspartate (NMDA) inhibitor) and tacrine, donepezil, galantamine, and rivastigmine (acetylcholinesterase inhibitors) are used to alleviate AD symptoms.

The indole nucleus is not only limited to pharmaceutical research and biological systems, but it is also a common moiety in material science (organic photovoltaic devices)[31] and agricultural applications, including fungicidal efficiency,[32] plant growth regulators,[33] and spore formation,[34] and has been used in industrial applications in dyes,[35] flavour enhancers,[36] food supplements,[37] fragrances, and photographic materials.[38]

Several indole alkaloids are effective anti-cholinesterase and memory enhancers, and therefore, they are intriguing candidates for anti-AD drug development.[39] The reported indole-based sulfonamide derivatives **1** have exhibited potent inhibition (IC_{50} = 0.17 ± 0.02 to 8.53 ± 0.32 μM) against acetylcholinesterase enzyme under the positive control of donepezil (IC_{50} = 0.014 ± 0.01 μM) as a standard drug.[21] It has been reported that the anti-cholinesterase potency of bis-indolyl imine **2** is the highest, with a percentage inhibition value of 89.21 ± 1.39 and 96.06 ± 1.41 at 200 μM, which is higher than that of standard galantamine for AChE (78.76 ± 0.94) and BChE (79.72 ± 0.33), respectively.[40] Bingul *et al.* reported the synthesis and anticholinesterase activity of novel indole-2-carbohydrazides **3a–d** and

[a]*Institute of Chemistry, Ibn e Sina Block, University of Sargodha, Sargodha-40100, Pakistan. E-mail: rauf.raza@uos.edu.pk; humaira.yasmeen@uos.edu.pk; sobiatariq66@gmail.com; shahzaibakhter740@gmail.com; muhammad.fayyaz@uos.edu.pk; Tel: +92-48-9230-546*

[b]*Department of Chemistry, Division of Science and Technology, University of Education, Lahore-54770, Pakistan. E-mail: laila.rubab@ue.edu.pk*

† Electronic supplementary information (ESI) available. See DOI: https://doi.org/10.1039/d2ra05105b

2-(indol-2-yl)-1,3,4-oxadiazoles **4a–d**. The % inhibition shown by these compounds is in the range of 36.85 ± 0.20 to 90.60 ± 1.56 at 200 μg cm^{-3} concentration compared with standard galantamine.[41]

2. Results and discussion

Our research goal is to synthesize enantiopure heterocycles following the Chiron approach of asymmetric synthesis. We have successfully synthesized and reported a number of enantiomerically pure fused heterocycles.[42,43] In considering the biological and other importance of natural and synthetic indoles, our goal is to produce indolic diazepine derivatives **36a–p** and determine their pharmacological potential (Scheme 1).

The synthetic strategy (Scheme 2) starts with the reaction of commercially available 3,5-dimethoxyaniline **5** or 3,4,5-trimethoxyaniline **6** with benzoin **7** (±-2-hydroxy-1,2-diphenyl ethanone) or acetoin **8** (±-3-hydroxy butan-2-one) to afford indoles **9–12** following a modified Bischler indole protocol.[44–46] The substituted indoles **9–12** would be formylated, following the Vilsmeier–Haack sequence (the addition of $POCl_3$ to DMF under anhydrous conditions to produce chloroiminium ion as an intermediate) to furnish indole aldehydes **13–16**. The resulting indole aldehydes **13–16** would be coupled with substituted anilines **17a–d** to produce indole imines (Schiff bases) **18a–p**. The C=N of these imines **18a–p** may be reduced with $NaBH_4$, preferably to result in the formation of indole amines **19–34**. The resulting amines **19–34** are a satisfactory synthon in our hand, and may be used in the formation of a variety of indolo-fused-diazepines **36a–p** or **37a–p** and indolo-fused-diazines **38a–p** (Scheme 2). The work on all three indole-based targets (**36–38**) is in progress in our laboratory.

The bathochromic shift in λ_{max} of the synthesized indoles (**9–12**), the appearance of an N–H as a single spike at 3353 ± 10 cm^{-1}, and the disappearance of any C=O stretching (corresponding to benzoin **7** or acetoin **8**) indicate the formation of

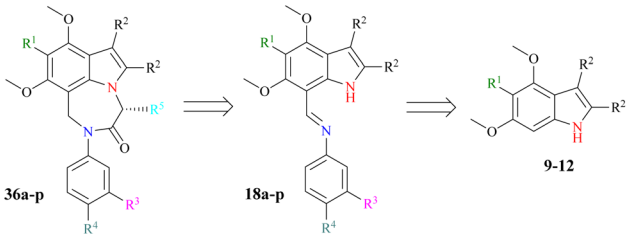

Scheme 1 Retrosynthesis of designed indole-based diazepines **36a–p**.

the indolic ring. Both indoles (**9** and **11**) are obtained as colourless crystalline solids. The low λ_{max} values of indoles (**9** and **11**) indicate that both phenyl rings at position 2 and 3 are not in conjugation with the remainder of the indolic chromophore. In fact, both phenyl groups are oriented perpendicular to the chromophore of the indole ring to minimize steric repulsion, which is supported by single crystal XRD studies (Fig. 1 and Table 1).

The molecular ion of indoles (**9** and **11**) does not undergo considerable fragmentation, indicating high stability due to high resonance energy. The $[M]^{+\bullet}$ appears as a base peak in the EIMS, which verifies the construction of the indolic ring. The ESI MS of indole **11** showed $[M + Na]^{+\bullet}$ at 382.1677 amu, which is clear evidence of the successful formation of the indole nucleus. The ^{1}H-NMR of indole **9** showed a pair of singlets (3.73 and 3.92 ppm) corresponding to the surrounding OMe groups, and two doublets of H^5 and H^7 appeared at 6.26 (J = 1.8 Hz) and 6.57 ppm (J = 1.8 Hz), respectively. The +R effect of OMe functionalities results in an upfield shift of H^5 and H^7. The aromatic protons of two phenyl rings emerged as multiplets of 10H integration. This concrete evidence was provided by single crystal XRD studies (Fig. 1 and Table 1).[47,48]

The indoles (**9** and **11**) were formylated by the reported Vilsmeier–Haack protocol, in which the formylating agent is the chloroiminium ion intermediate, generated by the interaction

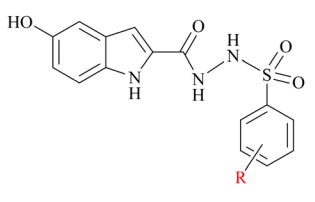

1 (R = F, Cl, Br, OMe, NO2, Me, CN)

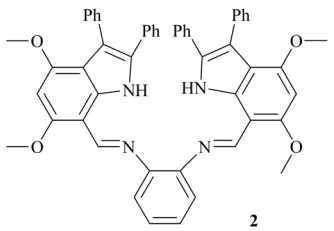

2

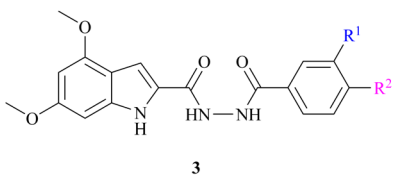

3

3-4	R^1	R^2
a	H	H
b	H	Me
c	H	NO_2
d	CF_3	H

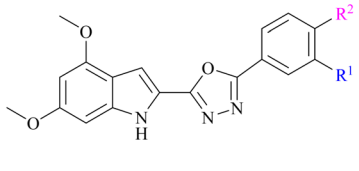

4

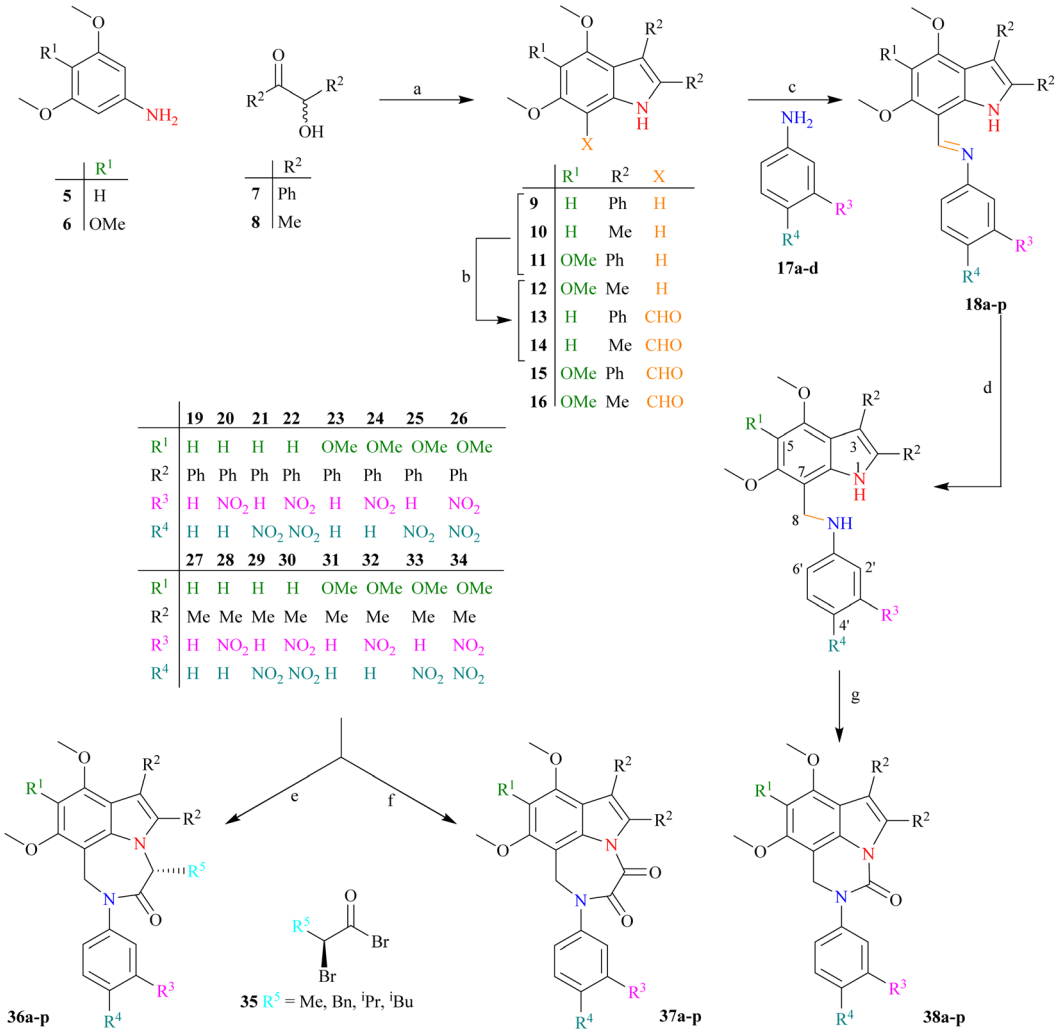

Scheme 2 (a) AcOH, $PhNH_2$ (cat.), 130 °C; (b) $POCl_3$, Me_2NCHO, ambient; (c) EtOH, reflux; (d) $NaBH_4$, dry THF/EtOH (3 : 1), reflux; (e) (i). LDA (−78 °C), (ii). **35**; (f) (i). LDA (−78 °C), (ii). $(COCl)_2$; (g) (i). LDA (−78 °C), (ii). $(MeO)_2CO$.

of DMF with $POCl_3$. No prominent change in the N–H stretching was observed between indoles **9** and **11** (3343 and 3363 cm^{-1}, respectively) and 7-formylindoles **13** and **15** (3298 and 3347 cm^{-1}, respectively) in the infra-red (IR) spectra, which suggests that no H-hydrogen bonding exists between formylic O and indolic H. The C=O bending in the 7-formylindoles (**13** and

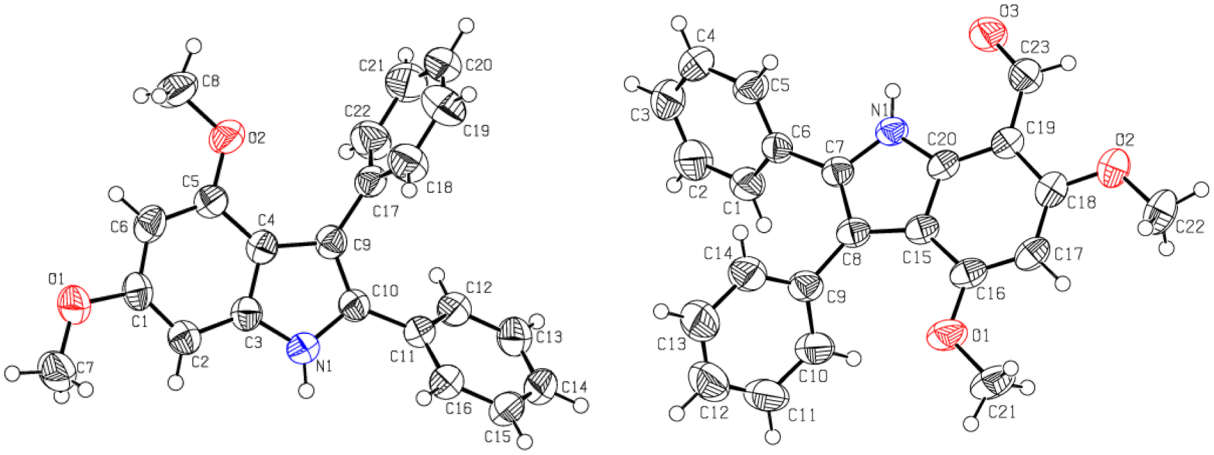

Fig. 1 The ORTEP presentations of 4,6-dimethoxy-2,3-diphenylindole **9** (left) and 7-formyl-4,6-dimethoxy-2,3-diphenylindole **13** (right).

Table 1 Selected crystallographic data for indole **9** and 7-formylindole **13**

Parameters	**9**	**13**
Molecular formula	$C_{22}H_{19}NO_2$	$C_{23}H_{21}NO_3$
Molecular mass (amu)	329.38	357.39
Crystal system, space group	Monoclinic, $P2_1/n$	Monoclinic, $P2_1/c$
Temperature (K)	296	296
a, b, c (Å)	11.7435 (16), 9.4480 (12), 15.940 (2)	32.036 (2), 7.2010 (4), 17.3062 (8)
α, β, γ (°)	90, 106.682 (7), 90	90, 112.060 (2), 90
Volume of crystal (Å^3)	1694.2 (4)	3700.1 (4)
Z	4	8
μ (MoKamm^{-1})	0.08	0.085
Crystal size (mm)	0.30 × 0.26 × 0.24	0.35 × 0.18 × 0.16

15) appears at a very low value (1608 and 1647 cm^{-1}, respectively), which reveals that the aldehydic functional group is attached to a highly conjugated system. The bathochromic shift in the λ_{max} of 7-formylindoles **13** and **15** (372, 358 nm, respectively) was observed in contrast to indoles **9** and **11** (322, 318 nm, respectively), which indicates an increase in conjugation due to the induction of a formyl moiety to the indolic chromophore.

The disappearance of doublets of H^7 in the aromatic region (6.57/6.78 ppm) along with the rise of other singlets at 10.41/10.43 ppm with no broadening upon D_2O exchange also indicated the formylation of indoles (**9** and **11**) to 7-formylindoles (**13** and **15**), respectively. The ^{13}C-NMR showed the C^5 and C^7 of indoles (**9** and **11**) as doublet and quaternary carbons, respectively, proving the occurrence of formylation at C^7. Furthermore, the doublet carbon of aldehydic functionality (H–C=O) arose at 188.2 and 190.0 ppm, respectively, in both indoles (**13** and **15**); the δ_H values indicate the connectivity of formyl functionality with a highly conjugated system. The −I effect of formyl functionality shifted C^7 to downfield. The single crystal XRD studies of 7-formylindoles (**13** and **15**) depict a perpendicular orientation of both phenyl groups, resulting in a minimum steric repulsion (Fig. 1 and Table 1).[47,48] The $[M]^{+\bullet}$ in the EIMS of both 7-formylindoles (**13** and **15**) is the base peak due to higher stability with no further considerable fragmentation.

The 7-formylindoles (**13** and **15**) would be condensed with a variety of substituted anilines **17a–d** to furnish a variety of indole imines **18a–p**, followed by the reduction of C=N to afford a variety of indole amines **19–34**. However, we limited ourselves to targeting the synthesis of the most potent (revealed after the *in silico* study) anti-cholinesterase indole amines (**20–22**, **24–26**). The *in silico* study revealed that the selected six indole amines (**20–22**, **24–26**) possessed great anti-cholinesterase potential. Interestingly, all six compounds contain NO_2 group(s) at either the *meta*-/*para*- or both positions in the aminic phenyl ring and two phenyl substituents at the 2- and 3-position of the indole ring.

The other similar indole amine derivatives (**28–30**, **32–34**) with two methyl groups at the 2- and 3-positions of the indole ring and a NO_2 group at either the *meta*- or *para*-position in the aminic phenyl ring exhibited a relatively low anti-cholinesterase potential with a relatively higher concentration of targeted indole amines (**20**, **21**, **24**, **25**) (Table 2 and S1†). Hence, only 2,3-diphenyl indole amines (**20–22**, **24–26**) were synthesized and characterized.

We attempted to synthesize eight derivatives of indole imines (**18a–h**) by coupling aniline **17a**/nitroanilines **17b–d** with 7-formylindoles (**13**/**15**). We already reported the synthesis of imines (Schiff bases) involving a variety of reagents; however, the reflux of anilines with 7-formylindoles in dry EtOH afforded the best yields.[48] Therefore, the coupling of nitroanilines **17b–d** with 7-formylindoles (**13**/**15**) was carried out by refluxing in dry EtOH.

It was observed that a longer reaction was required for the coupling of 7-formylindoles (**13**/**15**) with 4-nitroaniline **17c**, as compared to **17b**, which would be due to the −M effect of a *para*-NO_2 group that creates a positive charge on the *ipso*-C to NH_2 group. In fact, the lone pair on the NH_2 group exhibits poor basicity because it is delocalized from the NO_2 group, while in aniline **17b**, the lone pair on the NH_2 group is not delocalized from the NO_2 group. Surprisingly, the coupling of 3,4-dinitroaniline **17d** with 7-formylindoles (**13**/**15**) showed very poor transformation to the desired imines (**18d**, **18h**) while refluxing in dry EtOH for a week. This may be due to the strong −M effect of the *para*-NO_2 group and the reinforcing −I effect of the *meta*-NO_2 group.

Table 2 Binding energies (kcal mol^{-1} units) and dissociation constant (nanomolar units) values of targeted indole amines (**19–34**) revealed in the *in silico* study

Indole amines	R^1	R^2	R^3	R^4	Binding energy (kcal mol^{-1})	Dissociation constant (nM)
25	OMe	Ph	H	NO_2	−13.37	0.16
26	OMe	Ph	NO_2	NO_2	−12.81	0.4
24	OMe	Ph	NO_2	H	−12.43	0.77
22	H	Ph	NO_2	NO_2	−12.39	0.83
21	H	Ph	H	NO_2	−12.34	0.9
20	H	Ph	NO_2	H	−12.19	1.17
19	H	Ph	H	H	−11.67	2.81
23	OMe	Ph	H	H	−11.67	2.81
33	OMe	Me	H	NO_2	−10.3	28.02
30	H	Me	NO_2	NO_2	−10.21	32.58
34	OMe	Me	NO_2	NO_2	−9.93	52.58
29	H	Me	H	NO_2	−9.85	60.13
32	OMe	Me	NO_2	H	−9.57	97.32
28	H	Me	NO_2	H	−9.14	198.53
27	H	Me	H	H	−8.72	405.14

The two nitro groups on a phenyl ring caused additional electron withdrawal from the aminic (NH_2) group, decreasing its nucleophilicity (Scheme 3). We failed to synthesize two targeted indole imines (**18d**, **18h**), whereas the other four targeted indole imines (**18b**, **18c**, **18f**, **18g**) were successfully synthesized in excellent yield (76–88%) upon solidification from refluxing EtOH (Table 3). To crystallise these indole imines, a variety of solvents was used, but without success.

Four synthesized imines (**18b**, **18c** and **18f**, **18g**) showed no absorbance in the carbonyl (1600–1850 cm^{-1}) range, whilst a new signal at 1580 ± 4 cm^{-1} appeared in IR that indicated the transformation of C=O to C=NAr. Indolic N–H stretching was observed at 3333 ± 23 cm^{-1}. A slight bathochromic shift in the λ_{max} was exhibited by imines **18f**, **18g**, while a hypsochromic shift in the λ_{max} resulted for imines **18b**, **18c**, which indicated nothing. However, the presence of a singlet of most shielded aromatic protons (H^5) in only imines **18b**, **18c** and its absence in imines **18f**, **18g**, the appearance of an additional sharp singlet (did not show broadening upon D_2O exchange) at 9.06 ± 0.08 ppm, the appearance of a mostly deshielded new broad singlet (exhibited broadening upon D_2O exchange) at 11.12 ± 0.14 ppm in ^1H NMR, and upfield shifting of an aldehydic methine C (188.2 and 190.0 ppm) to an iminic methine C (158.0 ± 1.1 ppm) in ^{13}C NMR confirmed the formation of indole imines (**18b**, **18c** and **18f**, **18g**) (Table 3).

Because the synthesized indole imines (**18b**, **18c** and **18f**, **18g**) exist in an amorphous state, their single crystal XRD was not possible, although there were utmost efforts to crystallize these compounds with variable gradients. The single crystal XRD studies of *N*-phenyl(4,5,6-trimethoxy-2,3-diphenyl-1*H*-indol-7-yl)methanimine highlighted the perpendicular orientation of all three phenyl substituents and indicated the successful synthesis of the targeted compounds (Fig. 2 and Table S2†).

The reduction of imine **18b** to corresponding amine **20** was initially carried out under an H_2 atmosphere in the presence of a catalytic amount (5 mol%) of Pd(C), which resulted in the formation of a small amount of product. Prolonging the reaction duration improved nothing, which indicated that our imine **18b** acted as a bidentate ligand and coordinated with Pd [0] adsorbed on activated charcoal to result in transition metal complex **39** (Fig. 2). Alternatively, other common reducing agents such as $NaBH_4$ and $LiAlH_4$ were tried. A suspension of imine and $NaBH_4$ in MeOH was stirred at ambient temperature for an hour, but did not result in a reduction.

The excess $NaBH_4$ in dry EtOH : THF (1 : 1) solvent at ambient temperature resulted in incomplete conversion to products. Refluxing an imine and $NaBH_4$ in dry THF/EtOH (3 : 1) yielded amines **20**, **21** and **24**, **25**. The reduction with $LiAlH_4$ was useless, as it resulted in many inseparable products. The strong electron-releasing (+M) effect of OMe at indolic C^4 and C^6 rendered a prominent decrease in the electrophilicity of C=N, thus resulting in quite problematic reduction (Table 4).

The appearance of a signal of N–H at approximately 3368 ± 12 cm^{-1} in reduced candidates (**20**, **21**, **24** and **25**) as compared to their corresponding substrates (which displayed only one N–H absorption at 3333 ± 23 cm^{-1}) and the disappearance of a characteristic C=N absorption at approximately 1580 ± 4 cm^{-1} clearly indicated the successful reduction. The hypsochromic shift of λ_{max} from 368 ± 20 nm (imines) to 317 ± 3 nm was another clue as to the reduction of C=N functionality to C–N (Fig. 3).

The disappearance of a singlet of 1H corresponding to the iminic functionality (HC=N) at 9.06 ± 0.08 ppm and the appearance of a singlet of 2H integration corresponding to the amine (H_2C–NH) at 4.67 ± 0.02 ppm in ^1H-NMR confirmed the successful reduction of HC=N to H_2C–NH. The broad singlet of NH showed an upfield shift from 11.12 ± 0.14 ppm (imines) to 8.66 ± 0.03 ppm (reduced compounds), which is mainly due to the absorption in the anisotropic effect in later cases and a minor decrease in the electronegativity on N due to the change in hybridization from sp^2 to sp^3. The upfield shift of protons of aniline fragments also verified the conversion of HC=N to H_2C–NH due to a decrease in conjugation and reversal of the −M to +M effect of N.

The ^{13}C-NMR of indole amines verified the successful reduction of imines to amines, depicting the abolition of a doublet carbon of HC=N (C^8) at 158.0 ± 1.1 ppm and the emergence of a triplet C of H_2C–NH (C^8) at 40.7 ± 0.7 ppm. The upfield shift of aromatic protons in the indole amines compared to the indole imines also authenticated an increase in the +M effect of aminic N due to the transformation of HC=N into H_2C–NH (Fig. 4).

Utmost efforts were made to crystallize the targeted indole amines (**20**, **21**, **24** and **25**) with variable gradients, but were without success. Another derivative (4,5,6-trimethoxy-2,3-diphenyl-7-phenyl aminomethyl-1*H*-indole) was successfully crystallized from MeOH/$CHCl_3$. The single crystal XRD analysis of this indole amine indicated the successful reduction of the imine functional group to an amine (Fig. 5 and Table S3†).

2.1 *In silico* anti-cholinesterase activity

Initially, all the proposed compounds were virtually screened against acetylcholinesterase. In previous studies, it was observed that target ligands specifically interact either at the active catalytic site (CAS) or the peripheral anionic site (PAS) of

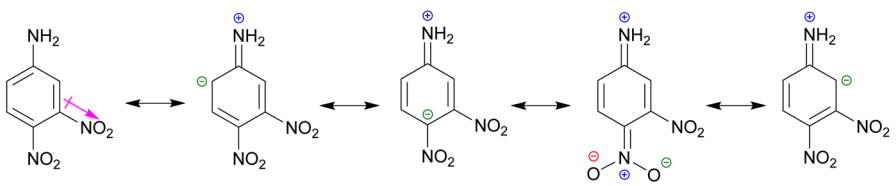

Scheme 3 The −M and −I effect of 4-nitro and 3-nitro groups, respectively, in aniline **17d** for decreasing its nucleophilicity.

Table 3 Selected spectroscopic data of indole imines (**18b**, **18c** and **18f**, **18g**)

Imine	% Yield	M.P. (°C)	λ_{max} (nm)	log ε^a (L.M^{-1} cm^{-1})	ν^b (cm^{-1})		δ^c (ppm)			
					C=N	N–H	HC=NAr	N–H	H^5	HC=NAr
18b	76	246	347	4.46683	1578	3310	9.13	11.26	6.22	157.2
18c	76	268	351	4.15902	1583	3345	9.14	11.25	6.23	158.9
18f	88	152	375	4.78249	1584	3356	9.10	11.14	—	156.9
18g	85	179	388	5.16388	1576	3350	8.96	10.98	—	159.1

[a] Recorded in MeOH. [b] Recorded as anhydrous KBr disc. [c] Recorded at 400 MHz NMR machine in $CDCl_3$.

acetylcholinesterase. The catalytic triad in CAS consists of Ser203, Glu334, and His447 surrounded by an anionic site with aromatic residues Trp86, Tyr130, Tyr337, and Phe338 involved in binding to the quaternary trimethylammonium choline moiety of ACh through cation–π interaction. The entrance of the catalytic gorge contains the peripheral anionic site (PAS) with Tyr72, Asp74, Tyr124, Trp286, and Tyr341 residues that allosterically perform catalysis. The CAS and PAS are connected by a narrow groove.[49]

The binding mode of the proposed indole amine **25** is characterized by a binding energy of −13.37 kcal mol^{-1} and a dissociation constant of 0.16 nM (Table 2). The hydrogen bonds of 3.68 and 3.01 Å with Asp74 of the PAS active site and 3.15 and 2.34 Å with Tyr337 of an anionic domain were observed in the stable binding. The –OH of Tyr337 and –OH from COOH of Asp74 formed a hydrogen bond with –NO_2 of compound **25**. The phenyl and pyrroline rings of indole amine **25** showed π–π stacking with Trp286 in the PAS region. The interaction of an indole moiety with Trp286 may lead to degenerative AChE activity.[50,51]

The following hydrophobic interactions occurred: phenyl ring with Gly292, Leu289, and Tyr72; the –CH_3 of methoxy groups with Val294, Phe338 (anionic domain), and Tyr341 (PAS); and phenyl ring of indole moieties with Gly121 (oxyanion hole) and Phe297 (acyl pocket) (Fig. 6). The acyl pocket (Trp236, Phe295, and Phe297) is involved in selective binding with ACh by stabilizing the acetyl group. The oxyanion hole consists of one water molecule and Gly121, Gly122, and Ala204 residues, which stabilize the negative transition state during acylation and deacylation.

Another proposed candidate, **24**, showed a binding energy of −12.43 kcal mol^{-1} with a dissociation constant of 0.77 nM against AChE (Table 2). Here, the oxygen atom of the methoxy group attached to the C2 atom of the phenyl ring of indole formed a hydrogen bond of 2.98 Å with the NH_2 of Phe295 in the acyl pocket of AChE. The oxygen atom of NO_2 at C28 of the phenyl ring of compound **24** formed a hydrogen bond of 3.69 Å with the NH_2 of Tyr124 located in the PAS, the allosteric binding site of AChE. The phenyl ring attached to the pyrroline and pyrroline ring formed π–π stacking with Trp286 of the PAS site (Fig. 7).

The indole amine **21** showed a binding energy of −12.34 kcal mol^{-1} with a dissociation constant of 0.9 nM against AChE (Table 2). The oxygen atom of NO_2 at C27

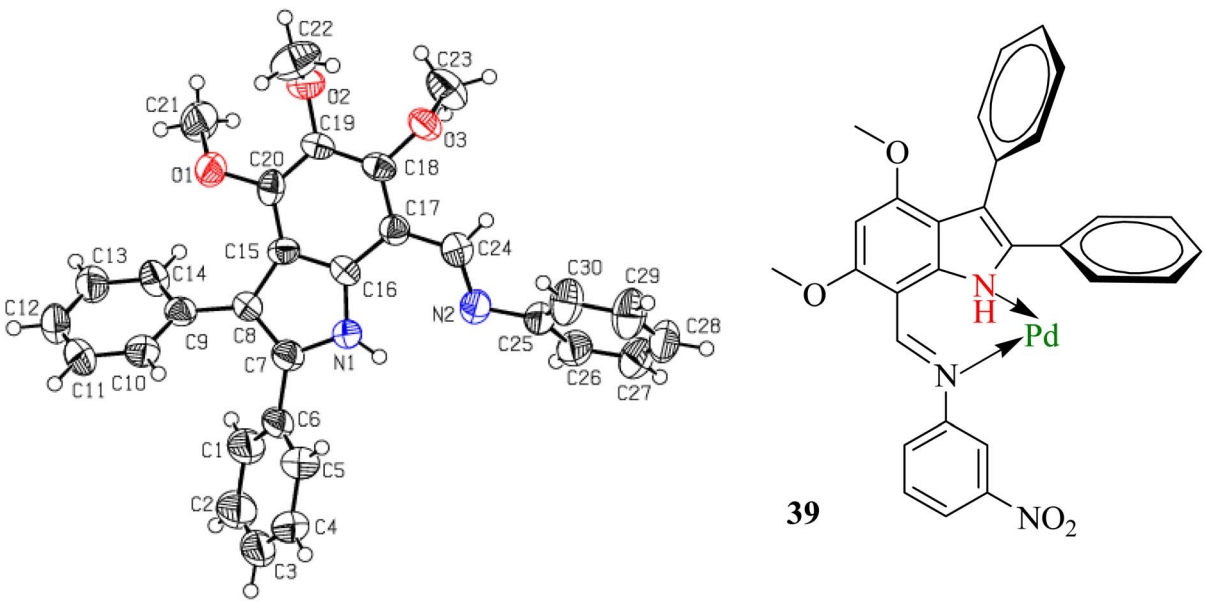

Fig. 2 The ORTEP presentation of *N*-phenyl(4,5,6-trimethoxy-2,3-diphenyl-1*H*-indol-7-yl)methanimine (left) and coordination of imine **18b** with Pd(C) to poison the catalyst.

Table 4 Trialed protocols for reducing imines (**18b**, **18c** and **18f**, **18g**) to amines (**20**, **21**, **24**, **25**)

	Reagents[a]	Temperature (Time in h)	Dry solvent	Product(s)	Yield
1	$NaBH_4$ (1.0 eq.)	rt (1)	MeOH	—	—
2	$NaBH_4$ (3.0 eq.)	rt (36)	MeOH	[b]	—
3	$NaBH_4$ (excess)	Reflux (3)	MeOH	[b]	—
4	$NaBH_4$ (excess)	Reflux (5–48)	THF : EtOH (3 : 1)	**20**	**86**
				21	**82**
				24	**89**
				25	**92**
5	$LiAlH_4$ (1.0 eq.)	rt (48)	THF : EtOH (3 : 1)	[b]	—

[a] Equivalents to respective imines. [b] mixture of reactant and product.

stabilized the docked complex by extensive hydrogen bonds of 3.03 and 3.73 Å with the OH of COOH in Asp74 of the PAS site and the H-bond of 3.19 Å with OH in the Tyr337 of anionic domain. Here, Trp286 also stabilized the docked complex by π–π stacking (Fig. 8).

A binding energy of −12.19 kcal mol^{-1} with a dissociation constant of 1.17 nM for indole amine **20** against AChE was found (Table 2). The carbonyl oxygen of COOH of Tyr341 in the PAS site formed a hydrogen bond of 3.75 Å with N1 of the pyrroline ring of **20**. The OH of COOH of Ser293 formed a hydrogen bond of 2.80 Å with the O4 of NO_2 in compound **20** in the acyl pocket of AChE. Here, Trp286 and Tyr341 formed π–π stacking with a phenyl ring attached to the indole moiety and the 4-NO_2 derivative phenyl ring of the compound (Fig. 9).

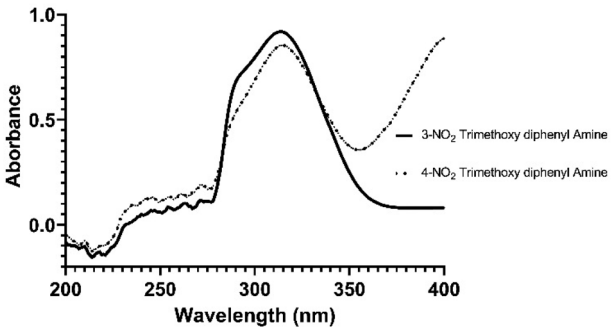

Fig. 4 The overlay UV spectra of indole amines **24** and **25** (recorded in MeOH at 26 °C).

2.2 *In vitro* anti-cholinesterase activity

The synthesized indole amines (**23**, **24** and **25**) were subjected to anti-acetylcholinesterase activity. Two amines (**24** and **25**) exhibited acetylcholinesterase inhibition comparable to that of galantamine, with IC_{50} values of 4.28 and 4.66 μM, respectively (Table 5). These inhibition potentials agree with the *in silico* results. The IC_{50} values of galantamine and donepezil were 4.15 and 0.028 μM, respectively, and are established cholinesterase inhibitors[52,53] that are being used as anti-AD therapeutics.[54,55] The natural indole amines (*e.g.*, serotonin) inhibit the acetylcholinesterase activity in plaques and tangles involved in the progression of AD.[56]

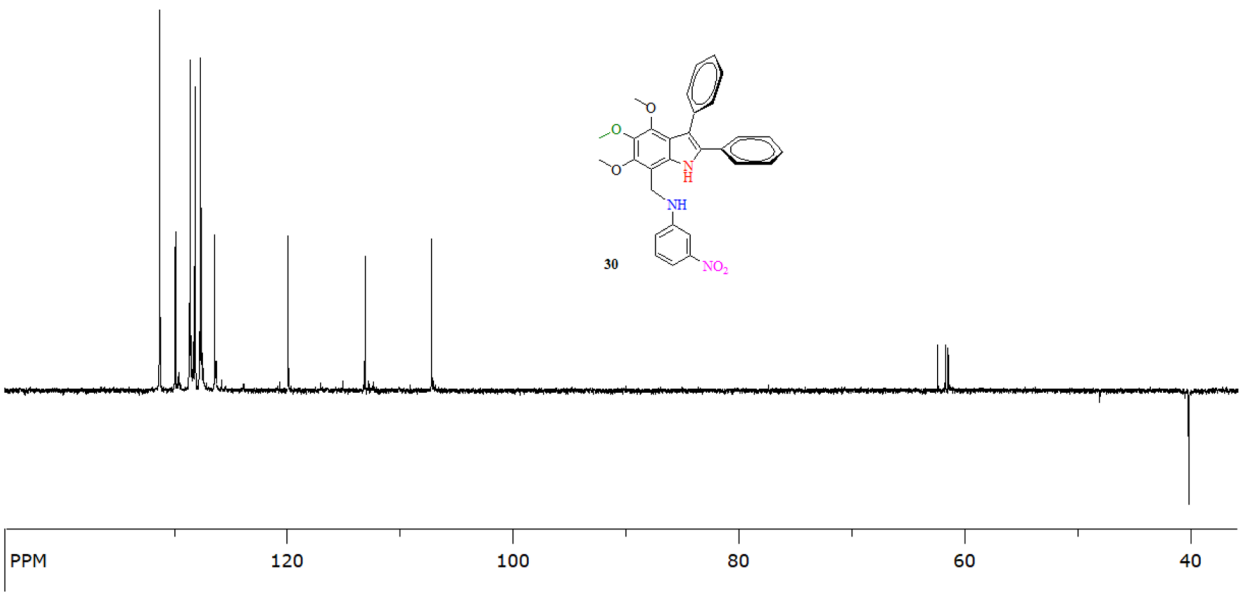

Fig. 3 The ^{13}C-NMR (DEPT-135°) of an indole amine **24** (at 100 MHz in $CDCl_3$) showing the presence of a methylene carbon (C^8) at 40.0 ppm.

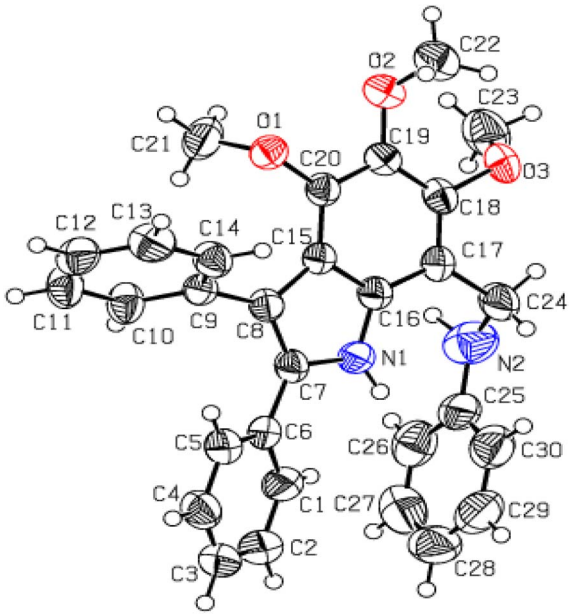

Fig. 5 The ORTEP presentation of 4,5,6-trimethoxy-2,3-diphenyl-7-phenylaminomethyl-1*H*-indole **23**.

2.3 ADMET parameters

Online web servers, including pkCSM (**https://structure.bioc.cam.ac.uk/pkcsm**) and SwissADME (**https://www.swissadme.ch/index.php**), were used to predict the absorption, distribution, metabolism, excretion, and toxicity (ADMET) properties of the novel synthesized indole derivatives. All synthesized indole-based derivatives have the highest intestinal absorption with high skin permeability as $\log K_p > -2.5$ cm h^{-1}. However, it was predicted that the Caco2 permeabilities of indole amines (**20**, **21**, **24** and **25**) were satisfactory, with Papp values greater than 0.90 cm s^{-1}.

All compounds were substrates of P-glycoprotein and were inhibitors of P-glycoprotein I and P-glycoprotein II. The indole amines (**24** and **25**) exhibited slightly low values of volume of distribution (V_d), while others showed the same values. All indole amines showed a fraction unbound value within the range of 0.239–0.312. The fraction unbound value represents compounds not bound to serum proteins, and thus, affects renal glomerular filtration and hepatic metabolism. If compounds show a high affinity for such proteins in the blood, they cannot cross the cell membrane.[57]

The indole amines (**24** and **25**) showed low values of blood–brain barrier (BBB) permeability. The BBB is the structure that controls the transfer of materials from blood to the brain and *vice versa*.[58] There were low values of central nervous system (CNS) permeability (log PS) for indole amines (**20** and **21**). All compounds were not substrates of CYP2D6 or CYP3A4. Each compound was an inhibitor of CYP1A2, CYP2C19, CYP2C9, CYP2D6, and CYP3A4 enzymes, which are the main cytochromes (CYP) in the P450 superfamily. The inhibition of CYP leads to the enhanced toxicity of drugs and decreases their efficacy.[59] The bioavailability of the drugs is related to hepatic and renal clearance in excretion. It is crucial for predicting the dosing rate of the drugs to study the steady-state concentration. All compounds showed total clearance within the range of 0.609–0.688 mL min^{-1} kg^{-1} (Table S4†).

3. Experimental

3.1 General information

All reagents (analytical grade) and chemicals were obtained from Sigma-Aldrich, Fluka, or Merck. Glass columns packed with silica gel (0.6–0.2 mm, 60 Å mesh size, Merck) were used for purification. Pre-coated silica gel (0.25 mm thick layer over

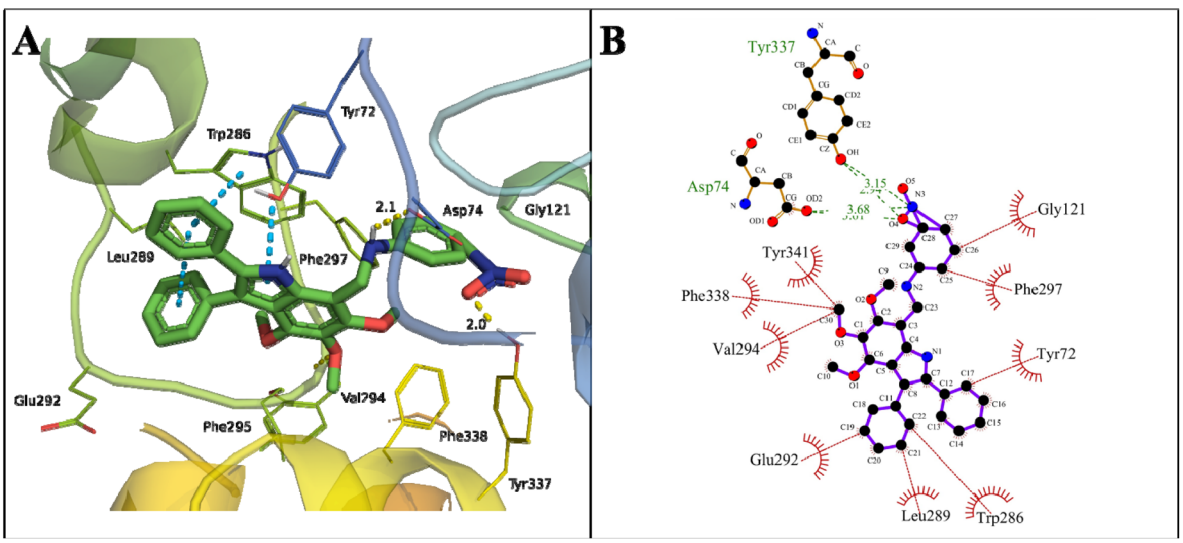

Fig. 6 Binding mode of indole amine **25** with AChE. (A) 3D interaction of key residues of 4M0E, where pi–pi stacking (blue dotted line), hydrogen bond (yellow dotted line), and π–cation (green dotted line) are represented. (B) 2D interaction of key residues of 4M0E, where hydrophobic interactions (red lines) and hydrogen bond (green lines) are represented.

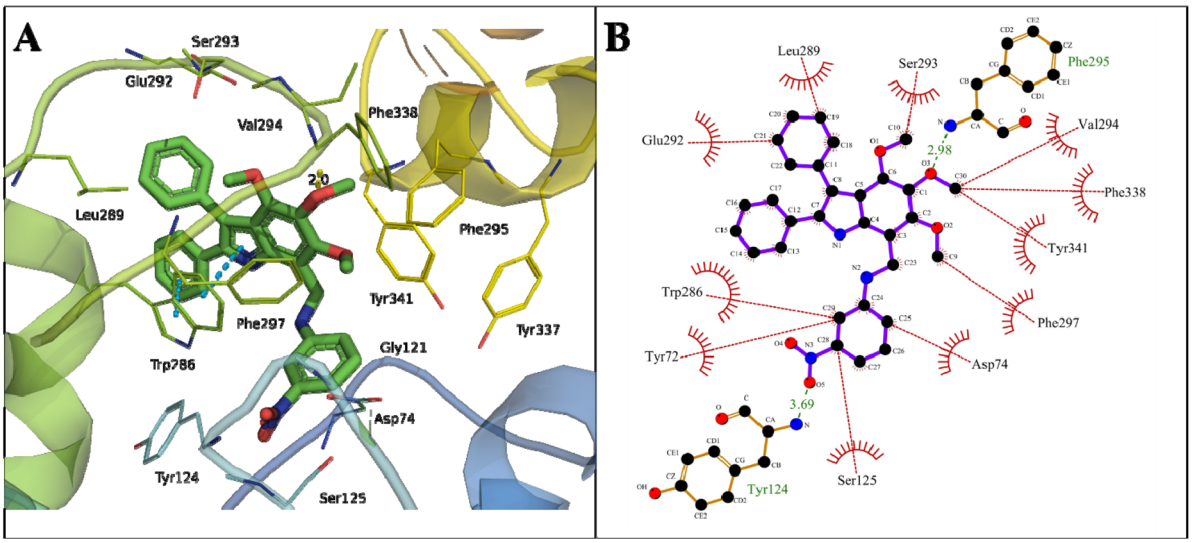

Fig. 7 Binding mode of indole amine **24** with AChE. (A) 3D interaction of key residues of AChE, where pi–pi stacking (blue dotted line), hydrogen bond (yellow dotted line), and π–cation (green dotted line) are represented. (B) 2D interaction of key residues of AChE, where hydrophobic interactions (red lines) and hydrogen bond (green lines) are represented.

Al sheet, Merck, Darmstadt, Germany) thin-layer chromatography (TLC) plates were used for reaction monitoring.

The Thermo Spectronic (UV-1700) spectrophotometer and Shimadzu (Prestige 21) FT-IR spectrometer were utilized for recording UV-Vis and IR spectra (as anhydrous KBr discs), respectively, at the High-Tech Laboratory, University of Sargodha, Sargodha (Pakistan). ^{1}H-NMR and ^{13}C-NMR were performed using a Bruker AVANCE DPX (300, 400, or 500 MHz) spectrometer in $CDCl_3$ at the ICCBS, H. E. J. Research Institute of Chemistry, University of Karachi, Karachi (Pakistan). For MS Q-TOF Ultima API (Micromass), the Biomedical Mass Spectrometry Facility (BMSF) at UNSW, Sydney (Australia) was utilized.

The single crystal XRD was performed using a Bruker Kappa APEX 11 CCD diffractometer at the University of Sargodha, Sargodha (Pakistan). Virtual screening for molecular docking and ADME prediction was performed using YASARA (Yet Another Scientific Artificial Reality Application) software version 20.7.4,[60] with a modified AutoDock LGA algorithm and AMBER03 force field and parameters that have been previously described. Docking poses were visualized and analysed by LigPlus[61] and PyMol software.

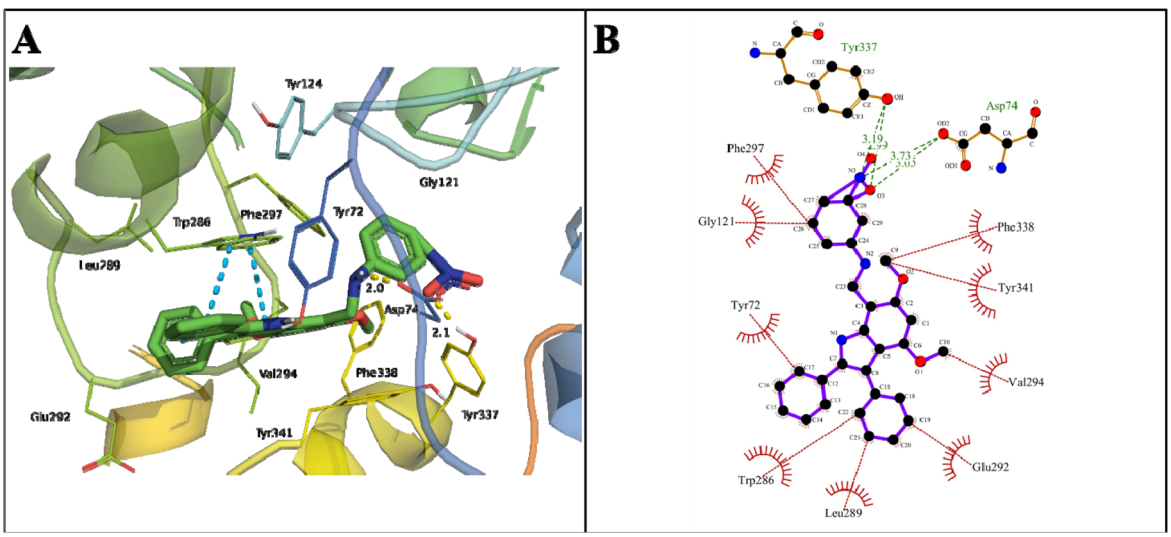

Fig. 8 Binding mode of indole amine **21** with AchE. (A) 3D interaction of key residues, where π–π stacking (blue dotted line), hydrogen bond (yellow dotted line), and π–cation (green dotted line) are represented. (B) 2D interaction of key residues of AChE with **21**, where hydrophobic interactions (red lines) and hydrogen bond (green lines) are represented.

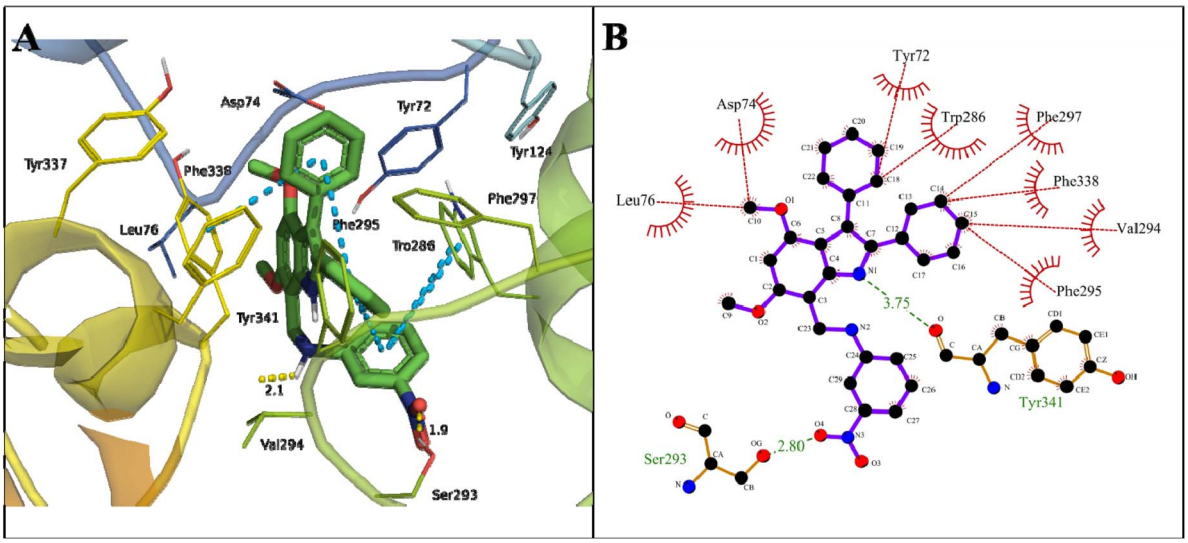

Fig. 9 Binding mode of indole amine **20** with AChE (4M0E). (A) 3D interaction of key residues of 4M0E, where pi–pi stacking (blue dotted line), hydrogen bond (yellow dotted line), and π–cation (green dotted line) are represented. (B) 2D interaction of key residues of 4M0E, where hydrophobic interactions (red lines) and hydrogen bond (green lines) are represented.

Table 5 *In vitro* inhibition of human serum acetylcholinesterase

	Indole amines	IC_{50}
1	**25**[a]	4.28 μM
2	**24**[a]	4.66 μM
3	**23**[b]	12.09 μM
4	Galantamine	4.15 μM
5	Donepezil	0.028 μM

[a] Precipitated at 10 μM concentration. [b] Precipitated at 15 μM concentration.

The pharmacokinetic properties and drug-likeness predictions for the top 10 compounds were performed by the SwissADME server (**https://www.swissadme.ch/**). The acetylcholinesterase inhibition was determined using a modification of the Ellman assay,[62] as described by Gholivand *et al.*[63]

A 96-well plate was used for the assay with 0.1 mM DTNB, 0.135 mM, acetylthiocholine iodide (AChI), and 70 mM phosphate-buffered saline (PBS) pH 7.4, for a total volume of 200 μL. In the reaction mixture, ATChI was added at the end to start the reaction. Positive and negative controls were also used. The absorbance was noted at 405 nm at 1 min intervals for at least ten minutes using a microwell plate reader (BioTek) at 25 °C. The reaction rates were calculated to obtain enzymatic activity and IC_{50}. All reactions were performed in triplicate. The ELISA reader ELx800 (BioTek, USA) and Gen5 3.02 software were used to calculate the absorbance of the solutions at variable wavelengths (in nm).

3.2 Synthesis of 2,3-diphenyl-(1*H*)-indoles (9, 11)

A mixture of aniline **5** or **6** (13.1 mmol, 3 eq.) with benzoin **7** (13.1 mmol, 3 eq.) was stirred at 120 °C for 2 h. The mixture was cooled to ambient temperature and stirred upon the addition of $PhNH_2$ (4.4 mmol, 1 eq.) and AcOH (8.1 mL, 8.5 g, 0.141 mol, 32 eq.). The resulting mixture was converted to a solution upon stirring (5 h) at 130 °C. Precipitation resulted after gradual cooling to ambient temperature. The precipitate was filtered, and the crude product was washed with chilled MeOH to afford a white solid (65–67%). A small portion of this amorphous solid was crystallized from EtOAc for spectroscopic and spectrometric characterization.

4,6-Dimethoxy-2,3-diphenyl-(1*H*)-indole 9. M. P. 240–242 °C.[48]

4,5,6-Trimethoxy-2,3-diphenyl-(1*H*)-indole 11. M. P. 218–220 °C.[48]

3.3 Synthesis of 2,3-diphenyl-(1*H*)-indole-7-carbaldehydes (13, 15)

The indole **9** or **11** (3 mmol, 1 eq.) was added to a stirred solution of $POCl_3$ (0.85 mL, 1.4 g, 9 mmol, 3 eq.) in DMF (20 mL) at ambient temperature. The resulting solution was stirred at room temperature for $2\frac{1}{2}$ h before being quenched with chilled H_2O (50 mL) and was basified with aq. NaOH solution (50 mL of 1 M). The resulting yellow precipitate was filtered, washed with chilled H_2O, and dried over anhydrous silica in a desiccator under reduced pressure to afford targeted aldehyde (80–92%) as a yellow amorphous solid. A small portion of this amorphous solid was crystallized from EtOAc/MeOH for spectroscopic and spectrometric characterization.

4,6-Dimethoxy-2,3-diphenyl-(1*H*)-indole-7-carbaldehyde 13. M. P. 180–182 °C.[48]

4,5,6-Trimethoxy-2,3-diphenyl-(1*H*)-indole-7-carbaldehyde 15. M. P. 158 °C.[48]

3.4 Synthesis of indole imines (18b, 18c, 18f, 18g)

The 4,6-dimethoxy-2,3-diphenyl-(1*H*)-indole-7-carbaldehyde **13** or 4,5,6-trimethoxy-2,3-diphenyl-(1*H*)-indole-7-carbaldehyde **15** (1.00/1.08 g, 2.8 mmol, 1 eq.) and aniline **17b** or **17c** (502 mg,

3.64 mmol, 1.3 eq.) were collectively dissolved in dry EtOH (25 mL). The resulting solution was refluxed for a variable duration until the disappearance of the aldehyde spot on the neutralized (after elution with *n*-hexane/Et_3N 1 : 1) TLC plate, which was chemically spotted with 2,4-dinitrophenylhydrazine (2,4-DNP) dip. The solvent was evaporated under reduced pressure, and the resulting solid product was flushed with chilled MeOH (3 × 20 mL) to afford an orange amorphous solid (**18b**, **18c**, **18f**, **18g**). It was attempted to further purify this orange solid by crystallization from different solvents without success.

***N*-(3′-Nitrophenyl) (4,6-dimethoxy-2,3-diphenyl-1*H*-indol-7-yl) methanimine 18b.** The imine **18b** was obtained as an orange solid (1.02 g, 76%); R_f: 0.48 (*n*-hexane/$CHCl_3$, 1 : 1); M.P. 268 °C; ν (cm^{-1}): 1578 (C=N), 3310 (N–H); log ε (λ_{max}, nm): 4.15902 (347); δ_H in ppm (500 MHz): 3.80, 3.99 (3H each, s, OCH_3), 6.22 (1H, s, H^5), 7.22–7.58 (12H, m, 3 Ph), 8.03 (1H, d, J = 7.8 Hz, $H^{4'}$), 8.10 (1H, t, J = 2.0 Hz, $H^{2'}$), 9.13 (1H, s, D_2O non-exchangeable, HC=N), 11.26 (1H, bs, D_2O exchangeable, NH); δ_C in ppm (125 MHz): 55.4, 56.5 (q, OCH_3), 87.5 (d, C^5), 101.7 (s, C^7), 113.0, 114.8 (s, C^3 & C^{3a}), 115.6 (d, $C^{5'}$), 119.5 (d, $C^{6'}$), 126.2, 127.1 (d, $C^{4''}$ & $C^{4'''}$), 127.5, 127.8, 128.6, 131.4 (all 2×, d, $C^{2''}$, $C^{3''}$, $C^{2'''}$ & $C^{3'''}$), 128.1 (d, $C^{4'}$), 129.7 (d, $C^{2'}$), 132.8, 133.0 (s, $C^{1''}$ & $C^{1'''}$), 135.7, 136.6 (s, C^2 & C^{7a}), 149.1 (s, $C^{3'}$), 154.2 (s, $C^{1'}$), 157.2 (d, C^8), 159.8, 160.2 (s, C^4 & C^6); CHNS analysis: found for $C_{29}H_{23}N_3O_4$: C (69.59%), H (4.57%), N (7.84%), requires: C (72.94%), H (4.85%), N (8.80%), O (13.40%).

***N*-(4′-Nitrophenyl) (4,6-dimethoxy-2,3-diphenyl-1*H*-indol-7-yl) methanimine, 18c.** The imine **18c** was obtained as a rusty yellow solid (1.175 g, 88%); R_f: 0.52 (*n*-hexane/$CHCl_3$, 1 : 1); M.P. 266 °C; ν (cm^{-1}): 1583 (C=N), 3345 N–H; log ε (λ_{max}, nm): 3.98706 (351); δ_H in ppm (500 MHz): 3.82, 3.98 (3H each, s, OCH_3), 7.08–7.29 (10H, m, 2 Ph), 7.36 (2H, d, J = 5.0 Hz, $H^{2'}$), 8.25 (2H, d, J = 5.0 Hz, $H^{3'}$), 9.14 (1H, s, D_2O non-exchangeable, HC=N), 11.25 (1H, bs, D_2O exchangeable, NH).

***N*-(3′-Nitrophenyl) (4,5,6-dimethoxy-2,3-diphenyl-1*H*-indol-7-yl)methanimine 18f.** The imine **18f** was obtained as a dark yellow solid (1.03 g, 77%); R_f: 0.62 (*n*-hexane/$CHCl_3$, 1 : 1); M.P. 168 °C; ν (cm^{-1}): 1584 (C=N), 3356 (N–H); log ε (λ_{max}, nm): 4.04059 (375); δ_H in ppm (500 MHz): 3.59, 3.88, 4.07 (3H each, s, OCH_3), 7.22–7.38 (12H, m, 2 Ph, $H^{5'}$ & $H^{6'}$), 7.40 (1H, d, J = 7.8 Hz, $H^{4'}$), 8.34 (1H, t, J = 2.0 Hz, $H^{2'}$), 9.10 (1H, s, D_2O non-exchangeable, HC=N), 11.14 (1H, bs, D_2O exchangeable, NH).

***N*-(4′-Nitrophenyl) (4,5,6-trimethoxy-2,3-diphenyl-1*H*-indol-7-yl)methanimine 18g.** The imine **18g** was obtained as a golden yellow solid (1.135 g, 85%); R_f: 0.51 (*n*-hexane/$CHCl_3$, 1 : 1); M.P. 179 °C; ν (cm^{-1}): 1576 (C=N), 3350 (N–H); log ε (λ_{max}, nm): 5.16388 (388); δ_H in ppm (500 MHz): 3.53, 3.84, 4.00 (3H each, s, OCH_3), 7.19–7.29 (10H, m, 2 Ph), 7.36 (2H, d, J = 5.0 Hz, $H^{2'}$), 8.25 (2H, d, J = 5.0 Hz, $H^{3'}$), 8.96 (1H, s, D_2O non-exchangeable, HC=N), 10.98 (1H, bs, D_2O non-exchangeable, NH); δ_C in ppm (125 MHz): 61.3, 61.5, 62.9 (q, OCH_3), 107.8 (s, C^7), 114.6, 118.7 (s, C^3 & C^{3a}), 121.8 (2×, d, $C^{2'}$), 125.2 (2×, d, $C^{3'}$), 127.6, 127.7 (d, $C^{4''}$ & $C^{4'''}$), 127.8, 127.9, 128.7, 131.2 (2×, d, $C^{2''}$, $C^{3''}$, $C^{2'''}$ & $C^{3'''}$), 131.2, 131.8 (s, $C^{1''}$ & $C^{1'''}$), 134.7, 135.4 (s, C^2 & C^{7a}), 145.4 (s, C^4/C^5/C^6), 153.2 (2×, s, any two of C^4, C^5 & C^6), 154.1 (s, $C^{4'}$), 159.1 (d of C^8 and s of $C^{1'}$ merged).

3.5 Reduction of imines to indole amines (20, 21, 24 and 25)

To a solution of indole imines (**18b**, **18c**, **18f**, **18g**) (1 mmol, 1 eq.) in THF/EtOH (3 : 1, 40 mL), $NaBH_4$ (151 mg, 4 mmol, 4 eq.) was added, and the suspension was refluxed for a variable duration. The solvent was partially removed under reduced pressure upon completion of the reaction (highlighted *via* TLC by the disappearance of imine's spot), and the reaction mixture was partitioned between chilled H_2O and $CHCl_3$ (3 × 30 mL). The combined organic layer was dried over anhydrous Na_2SO_4, rotary concentrated, and left standing overnight to afford indole amines (**20**, **21**, **24** and **25**) as a colourless solid in appreciable yield. The crystallization from different solvents failed.

4,6-Dimethoxy-7-(3′-nitrophenylaminomethyl)-2,3-diphenyl-(1*H*)-indole 20. M. P. 202 °C.[47]

4,6-Dimethoxy-7-(4′-nitrophenylaminomethyl)-2,3-diphenyl-(1*H*)-indole 21. M. P. 196 °C.[47]

4,5,6-Trimethoxy-2,3-diphenyl-7-phenylaminomethyl-(1*H*)-indole 23. M. P. 187 °C.[47]

4,5,6-Trimethoxy-7-(3′-nitrophenylaminomethyl)-2,3-diphenyl-(1*H*)-indole 24. Indole imine **18f** (507 mg); light yellow amorphous solid of indole amine **24** (453 mg, 89%); R_f: 0.65 (*n*-hexane/CH_2Cl_2, 3 : 2); M.P. 179 °C; ν (cm^{-1}): 3379 (N–H, broad s); log ε (λ_{max}, nm): 4.3613 (314); δ_H in ppm (400 MHz): 3.47, 3.96, 3.99 (3H each, s, OCH_3), 4.69 (2H, s, H^8), 7.05 (1H, dd, J = 8.2, 1.8 Hz, $H^{6'}$), 7.20–7.47 (14H, m, remainder of the signals of 3 Ph rings and aminic N–H), 8.69 (1H, bs, D_2O exchangeable, indolic N–H); δ_C in ppm (100 MHz): 40.0 (t, C^8), 61.3, 61.6, 62.2 (all q, OCH_3), 107.1 (d, $C^{6'}$), 108.4 (s, C^7), 113.0 (d, $C^{4'}$), 114.9 (s, C^{3a}), 118.9 (s, C^3), 119.8 (d, $C^{2'}$), 126.3 (d, $C^{5'}$), 127.5 (d, $C^{4'''}$), 127.6, 128.1, 128.5 (all 2×, d, $C^{2''}$, $C^{3'''}$ & $C^{2''}$), 129.8 (d, $C^{4''}$), 131.2 (2×, d, $C^{3''}$), 131.9, 132.3, 134.5, 135.3 (all s, $C^{1'''}$, $C^{1''}$, C^{7a}, C^2), 140.8 (s, $C^{1'}$), 147.1, 148.8, 149.2 (all s, C^4, C^5 & C^6), 149.3 (s, $C^{3'}$); HR ESIMS (*m*/*z*, amu): 510.2036 $[M + H]^+$.

4,5,6-Trimethoxy-7-(4′-nitrophenylaminomethyl)-2,3-diphenyl-(1*H*)-indole 25. Indole imine **18g** (507 mg); light yellow amorphous solid of indole amine **25** (468 mg, 92%); R_f: 0.51 ($CHCl_3$/*n*-hexane, 1 : 1); M.P. 191 °C; ν (cm^{-1}): 3356 (N–H, broad s); log ε (λ_{max}, nm): 4.2490 (320); δ_H in ppm (400 MHz): 3.53, 3.84, 4.00 (3H each, s, OCH_3), 4.65 (2H, s, H^8), 7.19–7.29 (11H, m, 2 Ph rings and aminic N–H), 7.41 (2H, d, J = 6.4 Hz, $H^{2'}$), 8.35 (2H, d, J = 6.4 Hz, $H^{3'}$), 8.63 (1H, bs, D_2O exchangeable, indolic N–H); δ_C in ppm (100 MHz): 41.3 (t, C^8), 61.0, 61.5, 62.9 (q, OCH_3), 107.8 (s, C^7), 110.4 (2×, s, $C^{2'}$), 114.9, 118.5 (s, C^3 & C^{3a}), 125.2 (2×, d, $C^{3'}$), 127.1, 128.2 (d, $C^{4''}$ & $C^{4'''}$), 127.6, 128.7, 129.7, 130.6 (2×, d, $C^{2''}$, $C^{3''}$, $C^{2'''}$ & $C^{3'''}$), 131.7, 132.9 (s, $C^{1''}$ & $C^{1'''}$), 135.5, 136.4 (s, C^2 & C^{7a}), 149.4 (2×, s, C^4 & C^6), 153.2 (s, C^5), 154.8 (s, $C^{1'}$), 158.8 (s, $C^{4'}$).

4. Conclusion

Our *in vitro* and *in silico* studies revealed that two indole amines (**24** and **25**) showed a strong acetylcholinesterase inhibition potential. These indole amines bind to the PAS site and may lead to enzyme inactivity. The IC_{50} values of reported compounds for acetylcholinesterase are comparable to the standard compound, galantamine. These can be further studied

for the development of cost-effective and one-step synthetic alternatives to current AD therapeutics.

Author contributions

Conceptualization, ARR and MFR; methodology, ST, SA, and SLR; software, MFR and SA; validation, ARR, SLR and HYG; formal analysis, SA and ST; investigation, SA, ST. and SLR; resources, MFR, ARR and SLR; writing—original draft preparation, HYG and MFR, and ARR; writing—review and editing, HYG, SA, MFR, and ARR; visualization, SA, MFR, and ARR; supervision, MFR and ARR; funding acquisition, ARR and MFR.

Conflicts of interest

The authors declare no conflicts of interest.

Acknowledgements

The authors acknowledge the Higher Education Commission (HEC) of Pakistan for generous financial support for research funding (HEC-20-3873). We are grateful to the University of Sargodha for the provision of basic instruments and the XRD facility.

References

1 A. S. Kuzmich, S. N. Fedorov, V. V. Shastina, L. K. Shubina, O. S. Radchenko, N. N. Balaneva, M. E. Zhidkov, J.-I. Park, J. Y. Kwak and V. A. Stonik, *Bioorg. Med. Chem.*, 2010, **18**, 3834–3840.
2 A. Andreani, S. Burnelli, M. Granaiola, A. Leoni, A. Locatelli, R. Morigi, M. Rambaldi, L. Varoli, L. Landi, C. Prata, M. V. Berridge, C. Grasso, H. H. Fiebig, G. Kelter, A. M. Burger and M. W. Kunkel, *J. Med. Chem.*, 2008, **51**, 4563–4570.
3 K. Lalit, B. Shashi and J. Kamal, *Int. J. Res. Pharm. Sci.*, 2012, **2**, 23–33.
4 L. Ding, J. Munch, H. Goerls, A. Maier, H. H. Fiebig, W. H. Lin and C. Hertweck, *Bioorg. Med. Chem. Lett.*, 2010, **20**, 6685–6687.
5 H. de Sousa Falcao, J. A. Leite, J. M. Barbosa-Filho, P. F. de Athayde-Filho, M. C. de Oliveira Chaves, M. D. Moura, A. L. Ferreira, A. B. de Almeida, A. R. Souza-Brito, M. de Fatima Formiga Melo Diniz and L. M. Batista, *Molecules*, 2008, **13**, 3198–3223.
6 F. Zhang, Y. Zhao, L. Sun, L. Ding, Y. Gu and P. Gong, *Eur. J. Med. Chem.*, 2011, **46**, 3149–3157.
7 S. T. Chan, A. N. Pearce, M. J. Page, M. Kaiser and B. R. Copp, *J. Nat. Prod.*, 2011, **74**, 1972–1979.
8 A. Longeon, B. R. Copp, E. Quevrain, M. Roue, B. Kientz, T. Cresteil, S. Petek, C. Debitus and M. L. Bourguet-Kondracki, *Mar. Drugs*, 2011, **9**, 879–888.
9 M. Verma, M. Tripathi, A. K. Saxena and K. Shanker, *Eur. J. Med. Chem.*, 1994, **29**, 941–946.
10 S. Cai, X. Kong, W. Wang, H. Zhou, T. Zhu, D. Li and Q. Gu, *Tetrahedron Lett.*, 2012, **53**, 2615–2617.
11 P. Devi, C. Rodrigues, C. G. Naik and L. D'Souza, *Indian J. Microbiol.*, 2012, **52**, 617–623.
12 Y. Takahashi, T. Kubota, A. Shibazaki, T. Gonoi, J. Fromont and J. Kobayashi, *Org. Lett.*, 2011, **13**, 3016–3019.
13 Y. Yamamoto and M. Kurazono, *Bioorg. Med. Chem. Lett.*, 2007, **17**, 1626–1628.
14 J. E. Macor, D. Gurley, T. Lanthorn, J. Loch, R. A. Mack, G. Mullen, O. Tran, N. Wright and J. C. Gordon, *Bioorg. Med. Chem. Lett.*, 2001, **11**, 319–321.
15 S. Biswal, U. Sahoo, S. Sethy, H. K. S. Kumar and M. Banerjee, *Asian J. Pharm. Clin. Res.*, 2012, **5**, 1–6.
16 N. Kumar, P. K. Sharma, V. I. K. Garg and P. Singh, *Curr. Res. Chem.*, 2011, **3**, 114–120.
17 M. S. Chambers, L. J. Street, S. Goodacre, S. C. Hobbs, P. Hunt, R. A. Jelley, V. G. Matassa, A. J. Reeve, F. Sternfeld and M. S. Beer, *J. Med. Chem.*, 1999, **42**, 691–705.
18 A. J. Kochanowska-Karamyan and M. T. Hamann, *Chem. Rev.*, 2010, **110**, 4489–4497.
19 H. P. Chang, M. L. Wang, M. H. Chan, Y. S. Chiu and Y. H. Chen, *Nutrition*, 2011, **27**, 463–470.
20 A. A. El-Gendy and H. A. El-Banna, *Arch. Pharmacal Res.*, 2001, **24**, 21–26.
21 M. Taha, F. J. Alshamrani, F. Rahim, N. Uddin, S. Chigurupati, N. B. Almandil, R. K. Farooq, N. Iqbal, M. Aldubayan and V. Venugopal, *J. King Saud Univ., Sci.*, 2021, **33**, 101401.
22 M. Bingul, S. Ercan and M. Boga, *J. Mol. Struct.*, 2020, **1213**, 128202.
23 M. Alomari, M. Taha, F. Rahim, M. Selvaraj, N. Iqbal, S. Chigurupati, S. Hussain, N. Uddin, N. B. Almandil and M. Nawaz, *Bioorg. Chem.*, 2021, **108**, 104638.
24 M. Taha, H. Ullah, L. M. R. Al Muqarrabun, M. N. Khan, F. Rahim, N. Ahmat, M. Ali and S. Perveen, *Eur. J. Med. Chem.*, 2018, **143**, 1757–1767.
25 M. Taha, M. S. Baharudin, N. H. Ismail, S. Imran, M. N. Khan, F. Rahim, M. Selvaraj, S. Chigurupati, M. Nawaz, F. Qureshi and S. Vijayabalan, *Bioorg. Chem.*, 2018, **80**, 36–42.
26 M. Taha, H. Ullah, L. M. R. Al Muqarrabun, M. N. Khan, F. Rahim, N. Ahmat, M. T. Javid, M. Ali and K. M. Khan, *Bioorg. Med. Chem.*, 2018, **26**, 152–160.
27 R. Pandey, K. V. Swamy and M. B. Khetmalas, *Ind. J. Biotech.*, 2013, **12**, 297–310.
28 L. Minati, T. Edginton, M. G. Bruzzone and G. Giaccone, *Am. J. Alzheimer's Dis. Other Dement.*, 2009, **24**, 95–121.
29 A. Alzheimer's, *Alzheimers. Dement.*, 2015, **11**, 332–384.
30 M. P. Mattson, *Nature*, 2004, **430**, 631–639.
31 Z. R. Owczarczyk, W. A. Braunecker, A. Garcia, R. Larsen, A. M. Nardes, N. Kopidakis, D. S. Ginley and D. C. Olson, *Macromolecules*, 2013, **46**, 1350–1360.
32 A. European Food Safety, *EFSA J.*, 2012, **10**, 2686.
33 I. M. Padilla, I. Vidoy and C. L. Encina, *Plant Cell Rep.*, 2009, **28**, 1411–1420.
34 K. Gerth, R. Metzger and H. Reichenbach, *Microbiology*, 1993, **139**, 865–871.
35 R. B. Mujumdar, L. A. Ernst, S. R. Mujumdar, C. J. Lewis and A. S. Waggoner, *Bioconjug. Chem.*, 1993, **4**, 105–111.

36 B. Stavric, B.-Y. Lau, T. I. Matula, R. Klassen, D. Lewis and R. H. Downie, *Food Chem. Toxicol.*, 1997, **35**, 185–197.
37 M. Suzui, M. Inamine, T. Kaneshiro, T. Morioka, N. Yoshimi, R. Suzuki, H. Kohno and T. Tanaka, *Int. J. Oncol.*, 2005, **27**, 1391–1399.
38 J. Buback, M. Kullmann, F. Langhojer, P. Nuernberger, R. Schmidt, F. Wurthner and T. Brixner, *J. Am. Chem. Soc.*, 2010, **132**, 16510–16519.
39 P. Williams, A. Sorribas and M.-J. R. Howes, *Nat. Prod. Rep.*, 2011, **28**, 48–77.
40 M. F. Saglam, M. Bingul, E. Şenkuytu, M. Boga, Y. Zorlu, H. Kandemir and I. F. Sengul, *J. Mol. Struct.*, 2020, **1215**, 128308.
41 M. Bingul, M. F. Saglam, H. Kandemir, M. Boga and I. F. Sengul, *Monatsh. Chem.*, 2019, **150**, 1553–1560.
42 B. Nisar, A. R. Raza, D. S. Black, N. Kumar and M. N. Tahir, *Chirality*, 2013, **25**, 865–870.
43 S. L. Rubab, B. Nisar, A. R. Raza, N. Ullah and M. N. Tahir, *Molecules*, 2013, **19**, 139–148.
44 D. S. Black, M. C. Bowyer, P. K. Bowyer, A. J. Ivory, M. Kim, N. Kumar, D. B. McConnell and M. Popiolek, *Aust. J. Chem.*, 1994, **47**, 1741–1750.
45 D. S. C. Black, N. Kumar and L. C. H. Wong, *Aust. J. Chem.*, 1986, **39**, 15–20.
46 D. S. C. Black, B. Gatehouse, F. Theobald and L. C. H. Wong, *Aust. J. Chem.*, 1980, **33**, 343–350.
47 S. Tariq, A. R. Raza, M. Khalid, S. L. Rubab, M. U. Khan, A. Ali, M. N. Tahir and A. A. C. Braga, *J. Mol. Struct.*, 2020, **1203**, 127438.
48 B. Nisar, S. L. Rubab, A. R. Raza, S. Tariq, A. Sultan and M. N. Tahir, *Mol. Diversity*, 2018, **22**, 709–722.
49 R. J. Kitz, L. M. Braswell and S. Ginsburg, *Mol. Pharmacol.*, 1970, **6**, 108–121.
50 N. C. Inestrosa, A. Alvarez, C. A. Perez, R. D. Moreno, M. Vicente, C. Linker, O. I. Casanueva, C. Soto and J. Garrido, *Neuron*, 1996, **16**, 881–891.
51 D. Barak, C. Kronman, A. Ordentlich, N. Ariel, A. Bromberg, D. Marcus, A. Lazar, B. Velan and A. Shafferman, *J. Biol. Chem.*, 1994, **269**, 6296–6305.
52 Z. Rakonczay, *Acta Biol. Hung.*, 2003, **54**, 183–189.
53 C. A. Barnes, J. Meltzer, F. Houston, G. Orr, K. McGann and G. L. Wenk, *Neuroscience*, 2000, **99**, 17–23.
54 L. Na-Young and K. Young-Sook, *Biomol. Ther.*, 2010, **18**, 65–70.
55 A. S. M. Ali Reza, M. S. Hossain, S. Akhter, M. R. Rahman, M. S. Nasrin, M. J. Uddin, G. Sadik and A. H. M. Khurshid Alam, *BMC Complementary Altern. Med.*, 2018, **18**, 123.
56 C. I. Wright, C. Guela and M. M. Mesulam, *Proc. Natl. Acad. Sci. U. S. A.*, 1993, **90**, 683–686.
57 R. Watanabe, T. Esaki, H. Kawashima, Y. Natsume-Kitatani, C. Nagao, R. Ohashi and K. Mizuguchi, *Mol. Pharmaceutics*, 2018, **15**, 5302–5311.
58 M. A. Malkiewicz, A. Szarmach, A. Sabisz, W. J. Cubala, E. Szurowska and P. J. Winklewski, *J. Neuroinflammation*, 2019, **16**, 15.
59 P. Manikandan and S. Nagini, *Curr. Drug Targets*, 2018, **19**, 38–54.
60 E. Krieger and G. Vriend, *Bioinformatics*, 2014, **30**, 2981–2982.
61 R. A. Laskowski and M. B. Swindells, *J. Chem. Inf. Model.*, 2011, **51**, 2778–2786.
62 M. Hoenicka, *Anal. Biochem.*, 1968, **25**, 192–205.
63 K. Gholivand, M. Abdollahi, F. Mojahed, A. M. Alizadehgan and G. Dehghan, *J. Enzyme Inhib. Med. Chem.*, 2009, **24**, 566–576.